Arabian Journal of Chemistry (2015) **xxx**, xxx–xxx

King Saud University

Arabian Journal of Chemistry

www.ksu.edu.sa
www.sciencedirect.com

ORIGINAL ARTICLE

Synthesis, characterization and electrochemical properties of copper(II) complexes derived from succinoyldihydrazine Schiff base ligands

R. Borthakur [a], A. Kumar [b], A.K. De [c], R.A. Lal [a,*]

[a] *Department of Chemistry, North Eastern Hill University, Shillong 793022, Meghalaya, India*
[b] *Department of Chemistry, Faculty of Science and Agriculture, The University of West-Indies, Augustine, Trinidad and Tobago*
[c] *Department of Science and Humanities, Tripura Institute of Technology, Narsingarh 799009, Tripura, India*

Received 1 March 2013; accepted 31 December 2014

KEYWORDS

Copper(II) complexes;
Succinoyldihydrazones;
Magnetic moment;
Spectroscopic studies

Abstract Four new copper(II) complexes of the composition $[Cu(H_2L)(H_2O)]$ have been synthesized by template method from reaction of copper(II) acetate, succinoyldihydrazine and some o-hydroxy aromatic aldehydes and ketones in aqueous methanol media. The composition of the complexes has been established on the basis of data obtained from analytical and mass spectral studies. The structure of the complexes has been discussed in the light of molar conductance, magnetic moment, Uv-vis, EPR and IR spectral studies. All of the complexes are non-electrolyte in DMSO. The μ_{eff} values for the complexes fall in the region 1.76–1.85 BM which rules out the possibility of any M–M interaction in the structural unit of the complexes. The ligands coordinate to the metal centre in enol form through phenolate/naphtholate oxygen atoms and azomethine nitrogen atoms. The NMR spectra show that ligands are present in anti-cis configuration in uncoordinated state. In all of the complexes the copper centre adopts square pyramidal stereochemistry. The unpaired electron is present in $d_{x^2-y^2}$ orbital in the ground state for copper centre in the complexes. The electron transfer reactions for the complexes have been studied by cyclic voltammetry.

1. Introduction

The copper complexes constitute an important class of molecules from several point of view viz. bioinorganic, catalysis and magnetism. Copper plays variety of roles in bioinorganic roles. Copper is an essential bio-element, responsible for numerous catalytic processes in living systems (Seigel and Siegel, 2002) where it is often present in different nuclearity. Copper is present in enzymes in biological systems either alone (Solomon et al., 2004) or in combination with

* Corresponding author. Tel.: +91 0364 2722616.
E-mail address: ralal@rediffmail.com (R.A. Lal).

Peer review under responsibility of King Saud University.

ELSEVIER Production and hosting by Elsevier

http://dx.doi.org/10.1016/j.arabjc.2014.12.040
1878-5352 Published by Elsevier Ltd.

some other metal ions (Gourlay et al., 2006) to discharge its function by redox reactivity.

All multicopper oxidases utilize at least four copper ions to couple the four electron reduction of O_2 to H_2O with four sequential one-electron substrate oxidation. Multicopper oxidases contain four copper ions: one blue copper or Type (1) site (T1) (Solomon et al., 1996), a normal or Type (2) site (T2) and a type (3) copper site (T_3) involving strong antiferromagnetic coupling leading to the lack of EPR signal. The T(2) and T(3) site form a trinuclear cluster which is the site for dioxygen reduction. On the other hand, T1 site is mononuclear in nature and its function is to transfer electrons from substrate to the trinuclear cluster.

Copper(II) complexes find applications as a catalyst for the oxidation of alcohols into aldehydes and ketones in organic chemistry with recognized industrial importance (Perez et al., 2012; Ajaikumar and Pandurangan, 2008). Among the newer, heterogeneous oxidation catalysts, copper containing porous material i.e. MOF present attractive interest (Xavier et al., 2004; Kato et al., 2005; Choudhary et al., 2004; Valodkar et al., 2004).

The dihydrazones are potential polyfunctional ligands capable of exhibiting keto-enol tautomerism. In particular, hydrazones derived from condensation of o-hydroxy aromatic aldehydes and ketones and variety of acid hydrazides give rise to condensed i.e. bi- and poly-nuclear complexes giving bridging via phenolic oxygen atoms (Ranford et al., 1998; Lalami et al., 2011; Chanu et al., 2012a,b; Lal et al., 2009). They are capable of giving rise to complexes having discrete molecularity as well as polymeric complexes through both the ligand as well as oxo-bridging because of their flexibility in three-dimensional space.

In the present study, we have selected the dihydrazones derived from condensation of succinoyldihydrazines and o-hydroxy-aromatic aldehydes. In succinoyldihydrazones, the two hydrazone parts are joined together through two methylene groups. These dihydrazones are examples of polyfunctional ligands and are unique in the sense that their succinoyl fraction offers greater flexibility in three dimensional space because of its capability for free rotation about C—C single bond as compared to those in which the two hydrazone groupings are joined together either directly (oxaloyl) or through phenyl or pyridyl groups. However, succinoyldihydrazones by virtue of their greater flexibility are expected to be more reactive ligands than those derived from oxaloyl, phenyl, pyridyl dihydrazones and to yield more stable complexes. The dihydrazones in the present study contain salicylaldimine, 5-bromo-salicylaldimine, acetophenimine dihydrazone and 2-hydroxy-1-naphthaldimine in their molecular skeleton. As we go from salicylaldimine dihydrazone to acetophenimine dihydrazone to naphthaldimine dihydrazone to 5-bromo-salicylaldimine dihydrazone, the bulkiness and electronegativity both increase in the same order.

A survey of literature reveals that although some isolated studies are available on metal complexes of succinoyldihydrazones and related dihydrazones (Ranford et al., 1998; Lalami et al., 2011; Chanu et al., 2012a,b; Lal et al., 2009; Dinda et al., 2003; John et al., 2007; Lal et al., 2010a), yet the systematic study on the synthesis and characterization of copper complexes of succinoyldihydrazones is absent in spite of their highly flexible nature. Moreover, the work on metal complexes of dihydrazones synthesized by template method and the elucidation of their structure is almost non-existent to the best of our knowledge except that by us (Kumar et al., 2011). Hence, in view of the above importance of copper complexes, absence of systematic work on metal complexes of dihydrazones synthesized by template method and highly flexible nature of succinoyl dihydrazones, it was of interest to synthesize the copper complexes of some succinoyl dihydrazones by template method and to characterize by various physicochemical and spectroscopic techniques and to study their electron transfer reactions. Accordingly, some copper complexes of the entitled succinoyldihydrazones (Fig. 1) have been synthesized and characterized. The results of such an investigation are presented in this paper.

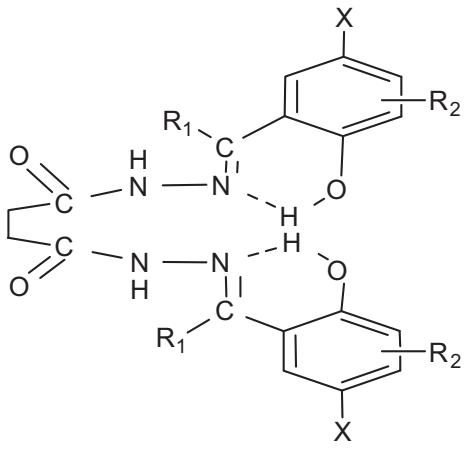

Figure 1 Structure of ligands.

2. Experimental

2.1. Materials and reagents

Copper acetate monohydrate, diethyl succinate, hydrazine hydrate, substituted salicylaldehyde and 2-hydroxy-1-naphthaldehyde were E-Merck, Qualigens, Hi-Media or equivalent grade reagents.

2.2. Instruments

Copper was estimated by standard literature procedure (Vogel, 1978). C, H, N were determined by microanalytical methods. The study of morphology was performed by JEOL-JSM 6360CX with tungsten filament using a Si (Li) detector with a resolution 3 nm. Samples were placed on a brass stubs and analysis was achieved at 20 kV of acceleration voltage and 10–270 Pa of adjustable pressure in the sample chamber. The metal coating of the samples were carried out under vacuum in an inert atmosphere using argon gas and used gold as a target of about 35 nm (350 Å). The images were obtained with the back scattering electron signal. Analyses were focused near the edge where the sample is thinner. Transmission electron microscopy images were measured on a JEOL-JEM-2100CX electron microscope operated at 200 kV without the addition of a contrast agent since the presence of the metal ion provided enough contrast. For TEM imaging, a drop of sample solution was cast out on carbon coated copper grid and allowed to dry.

Please cite this article in press as: Borthakur, R. et al., Synthesis, characterization and electrochemical properties of copper(II) complexes derived from succinoyldihydrazine Schiff base ligands. Arabian Journal of Chemistry (2015), http://dx.doi.org/10.1016/j.arabjc.2014.12.040

All conductance measurements were made at 1 kHz using Wayne Kerr B905 Automatic Precision Bridge. A dip-type conductivity cell having a platinised platinum electrode was used. The cell constant was determined using a standard KCl solution. Room temperature magnetic susceptibility measurements were made on a Sherwood Magnetic Susceptibility Balance MSB-Auto. Diamagnetic corrections were carried out using Pascals Constant (Syamal and Dutta, 1993). Electronic spectra of the complexes were recorded in DMSO solution at $\sim 10^{-3}$ M concentration on a Perkin–Elmer Lambda-25 spectrophotometer. ^{1}H and ^{13}C NMR spectra were recorded on a Bruker Avance II 400 and 100 MHz spectrometer in DMSO-d_6 using TMS as an internal standard. Electron paramagnetic resonance spectra of the complexes were recorded at X-band frequency on a Varian E-112 E-Line Century Service EPR spectrometer using TCNE (g = 2.0027) as an internal field marker. Variable temperature experiments were carried out with a Varian Variable Temperature accessory. Infrared spectra were recorded on a BX-III/FT-IR Perkin–Elmer Spectrophotometer in the range 4000–400 cm^{-1} in KBr discs. The molecular weights of the complexes were determined in DMSO by freezing point depression. Mass losses were determined by heating the complexes at 110 °C and 180 °C in an electronic oven. APCI mass spectra of the complexes were recorded on a water Zg 4000 Micromass Spectrometer using DMSO as a solvent. Cyclic voltammetric measurements of the compounds in DMSO were done using a CH instruments electrochemical analyzer under dinitrogen. The electrolytic cell comprises of three electrodes, the working electrode was a Pt disc while the reference and auxiliary electrodes were Ag/AgCl separated from the sample solution by a salt bridge and a Pt wire, respectively; 0.1 mol L^{-1}, TBAP was used as the supporting electrolyte.

2.3. Synthesis of ligands

Succinoyldihydrazine was prepared by reacting diethyl succinate (10.0 g, 49.50 mmol) with hydrazine hydrate (5.50 g, 110.00 mmol) under reflux for 4 h and recrystallized from methanol. Dihydrazones were prepared by reacting a solution of succinoyldihydrazine (10.37 mmol) in methanol with aldehyde/ketones (25.93 mmol) in hot methanol and refluxing the reaction mixture for 30 min. The precipitate obtained on cooling the solution was thoroughly washed with methanol and air dried.

H_4L^1: Colour: White; Yield: 89%; M.p.: 250 °C; Anal. Calc. for $C_{18}H_{18}N_4O_4$ (354 g mol^{-1}): C, 61.02; H, 5.08; N, 15.82. Found: C, 61.23; H, 5.06; N, 15.69; ^{1}H NMR (400 MHz, DMSO-d_6) (δ ppm): 11.72 (d, 1H, J = 7.6 Hz, OH), 11.30 (d, J = 5.2 Hz, 1H, OH), 11.16 (s, 1H, NH), 10.15 (s, 1H, NH), 8.33 (s, 1H, CH═N), 8.27 (s, 1H, CH═N), 6.8–7.6 (m, 8H, Ar—H), 2.91 (m, 2H), 2.53 (m, 2H); ^{13}C NMR (100 MHz, DMSO-d_6) (δ ppm): 26.5, 27.2, 116.1, 116.3, 119.2, 119.4, 126.7, 129.4, 130.8, 130.9, 140.8, 140.9, 146.2, 146.3, 156.3, 157.3, 167.2, 167.6.

H_4L^2: Colour: Light yellow; Yield: 87%; M.p.: 257 °C; Anal. Calc. for $C_{18}H_{16}N_4O_4Br_2$ (512 g mol^{-1}): C, 42.19; H, 3.13; N, 10.94. Found: C, 42.59; H, 3.11; N, 11.24. ^{1}H NMR (400 MHz, DMSO-d_6) (δ ppm): 11.75 (d, 1H, J = 7.8 Hz, OH), 11.36 (d, 1H, J = 4.8 Hz, OH), 11.19 (s, 1H, NH), 10.2 (s, 1H, NH), 8.30 (s, 1H, CH═N), 8.21 (s, 1H, CH═N), 6.8–7.7 (m, 6H, Ar—H), 2.92 (m, 2H), 2.53 (m, 2H); ^{13}C NMR (100 MHz, DMSO-d_6) (δ ppm): 26.4, 27.1, 110.3, 110.7, 118.3, 118.5, 130.4, 130.5, 133.1, 133.3, 138.3, 138.4, 143.7, 143.8, 155.4, 156.2, 167.8, 168.1.

H_4L^3: Colour: Light yellow; Yield: 85%; M.p.: 238 °C; Anal. Calc. for $C_{20}H_{22}N_4O_4$ (382 g mol^{-1}): C, 62.83; H, 5.76; N, 14.66. Found: C, 62.98; H, 5.74; N, 14.86. ^{1}H NMR (400 MHz, DMSO-d_6) (δ ppm):13.24 (d, 1H, J = 7.6 Hz, OH), 12.97 (d, 1H, J = 5.1 Hz, OH), 11.09 (s, 1H, NH), 10.2 (s, 1H, NH), 6.8–7.7 (m, 8H, Ar—H), 3.83 (s, 3H), 2.75 (s, 3H), 2.53 (m, 2H), 2.34 (m, 2H); ^{13}C NMR (100 MHz, DMSO-d_6) (δ ppm): 13.1, 28.4, 28.8, 114.9, 117.1, 117.2, 117.9, 118.5, 119.0, 127.5, 128.9, 130.4, 132.4, 153.7, 158.6, 168.3, 168.4.

H_4L^4: Colour: Dark yellow; Yield: 86%; M.p.: 245 °C; Anal. Calc. for $C_{26}H_{22}N_4O_4$ (454 g mol^{-1}): C, 68.72; H, 4.83; N, 12.33. Found: C, 68.99; H, 4.83; N, 12.65. ^{1}H NMR (400 MHz, DMSO-d_6) (δ ppm):12.66 (d, 1H, J = 14.4 Hz, OH), 11.62 (d, 1H, OH), 11.3 (s, 1H, NH), 10.05 (s, 1H, NH), 9.17 (s, 1H, CH═N), 8.98 (s, 1H, CH═N), 7.18–8.44 (m, 12H, Ar—H), 2.59 (m, 2H), 2.07 (m, 2H); ^{3}C NMR (100 MHz, DMSO-d_6) (δ ppm): 25.1, 27.5, 118.3, 118.6, 121.9, 122.0, 123.3, 124.1, 127.5, 127.7, 128.7, 128.8, 131.5, 131.7, 144.8, 157.7, 163.9, 167.3 127.5, 127.7, 128.7, 128.8, 132.3, 138.3, 163.9, 167.3.

2.4. Synthesis of the complexes

2.4.1. Preparation of $[Cu(H_2L^n)(H_2O)]$ (H_4L^n = H_4L^1, H_4L^2, H_4L^3, H_4L^4)

Succinoyldihydrazine (SDH) (1.00 g, 6.85 mmol) was dissolved in H_2O (20 mL). To this solution, $Cu(OAc)_2 \bullet H_2O$ (1.37 g, 6.87 mmol) dissolved in methanol (60 mL) was added slowly accompanied by gentle stirring and the resulting solution was stirred for 10 min. This solution was then added drop by drop to salicylaldehyde solution (2.09 mL, 20.61 mmol) in methanol (150 mL) over a period of 30 min accompanied by vigorous stirring. This precipitated a green coloured compound which was refluxed for half an hour, then filtered, washed three times with methanol (30 mL each time) followed by ether and finally dried over anhydrous $CaCl_2$.

The complexes $[Cu(H_4L^2)(H_2O)]$ (**2**), $[Cu(H_4L^3)(H_2O)]$ (**3**) and $[Cu(H_4L^4)(H_2O)]$ (**4**) were also prepared by following the above procedure using 5-bromosalicylaldehyde (4.14 g, 20.61 mmol), 2-hydroxyacetophenone (1.37 g, 20.61 mmol) and 2-hydroxy-1-naphthaldehyde (2.95 g, 20.61 mmol) respectively, instead of salicylaldehyde.

$[Cu(H_2L^1)(H_2O)]$ (**1**): Yield: 2.60 g (78%), M.p.:200 °C *Anal*: *Calc for* $C_{18}H_{18}N_4O_4Cu$ (433.54 g mol^{-1}): Cu, 14.27; C, 50.23; H, 4.12; N, 13.30. Found: Cu, 14.66; C, 44.82; H, 4.15; N, 12.91. Molar Conductance (DMSO, Ω^{-1} cm^2 mol^{-1}): 0.8.

$[Cu(H_2L^2)(H_2O)]$ (**2**): Yield: 2.45 g (85%), M.p.:240 °C *Anal*: *Calc for* $C_{18}H_{16}N_4O_4\ Br_2Cu$ (591.54 g mol^{-1}): Cu, 10.35; C, 36.18; H, 2.67; N, 9.89. Found: Cu, 10.74; C, 36.51; H, 2.70; N, 9.47. Molar Conductance (DMSO, Ω^{-1} cm^2 mol^{-1}): 0.5.

$[Cu(H_2L^3)(H_2O)]$ (**3**): Yield: 2.20 g (76%), M.p.:230 °C *Anal*: *Calc for* $C_{20}H_{22}N_4O_4Cu$ (461.54 g mol^{-1}): Cu, 13.38; C, 52.27; H, 4.75; N, 12.41. Found: Cu, 13.77; C, 51.99; H, 4.77; N, 12.11. Molar Conductance (DMSO, Ω^{-1} cm^2 mol^{-1}): 0.3.

Please cite this article in press as: Borthakur, R. et al., Synthesis, characterization and electrochemical properties of copper(II) complexes derived from succinoyldihydrazine Schiff base ligands. Arabian Journal of Chemistry (2015), http://dx.doi.org/10.1016/j.arabjc.2014.12.040

[Cu(H_2L^4)(H_2O)] (**4**): Yield: 2.23 g (72%), M.p.:234 °C *Anal*: *Calc for* $C_{26}H_{22}N_4O_4Cu$ (533.54 g mol^{-1}): Cu, 11.56; C, 58.82; H, 4.10; N, 10.32. Found: Cu, 11.95; C, 54.48; H, 4.12; N, 10.50. Molar Conductance (DMSO, Ω^{-1} cm^2 mol^{-1}): 0.7.

3. Result and discussion

3.1. Characterization of dihydrazones

Two proton signals observed in the region δ11.30–13.25 ppm are assigned to δ(OH) protons while the other two proton signals in the region δ10.05–11.21 ppm are assigned to δ(NH) protons. The signals in the region δ8.21–9.18 ppm are assigned to the azomethine (—CH═N) protons in all the uncoordinated dihydrazones except H_4L^3, which shows a ketonic methyl proton signal at δ3.38 ppm. A multiplet in the region δ6.87–8.44 ppm is assigned to phenyl and naphthyl protons. Further, the two signals observed in the region δ δ2.37–2.93 ppm are assigned to methylene protons (Jackman and Sternhell, 1978). The two methylene protons appear at different fields which is consistent with their different chemical environment in the ligand.

The signals in the region δ2.65–2.93 ppm are attributed to the methylene protons (a) close to the carbonyl oxygen, while the signals in the region δ2.37–2.53 ppm are attributed to the methylene proton (b) distant from carbonyl oxygen. The signals in the region δ11.30–13.25 ppm and δ9.99–11.14 ppm for the ligands appear as either two singlets or two doublets. The signals in the region δ8.21–9.18 ppm appear in the form of two resonances only. If the dihydrazones exist in the syn-cis or staggered configuration, the δOH. δNH and δ(—CH═N—) resonances should appear as a singlet. On the other hand, if the δOH, δNH and δ(—CH═N—) resonances show multiplicity, the dihydrazones should exist in the anti-cis configuration. The appearance of the δOH, δ(—CH═N—) and δNH proton resonances in the form of either two singlets or two doublets for the ligands suggests the existence of dihydrazones in the anti-cis configuration.

The existence of these ligands in the *anti-cis* configuration is attributed to strong intramolecular and intermolecular hydrogen bonding which inhibits free rotation of the hydrazone groupings around the C—C bond. As a result of this anti-cis configuration of the ligands one of the hydrazone groupings attains an axial position while the other hydrazone grouping remains in the equatorial plane. Consequently, the equatorial protons appear upfield as compared to the axial protons. Further, coupling between the axial and the equatorial protons ultimately leads to splitting of their signals. Consequently, the δ(OH) and δ(NH) signals appear in the form of two doublets while the δ(—CH═N—) signals appear in the form of two resonances only.

The dihydrazones H_4L^1–H_4L^3 contain eighteen number of carbon atoms each while the dihydrazone H_4L^4 contains twenty-six numbers of carbon atoms. The number of ^{13}C NMR signals observed in uncoordinated ligands is the same as the number of carbon atoms in each of the ligands i.e. 18, 18, 18 and 26, respectively. The existence of same number of signals in the ^{13}C NMR spectra of ligands as the number of carbon atoms suggests that all of the carbon atoms are not in the same plane in solution. This is possible only if the

Table 1 Complex, colour, decomposition point, elemental analysis, molar conductance and electronic spectral data for Cu(II) complexes derived from succinoyldihydrazones.

Sl. No.	Complex and colour	M.P. (°C)	Molecular weight	Elemental analysis: found (calcd)				Molar conductance	Electronic spectral bands λ_{max} (nm), ε_{max} (dm^3 cm^{-1} mol^{-1})[a]	
				Cu	C	H	N		Solid	Solution
1	[Cu(H_2L^1)(H_2O)] (1) green	200	480 ± 15(433.54)	14.27 (14.66)	50.23 (49.82)	4.12 (4.15)	13.30 (12.91)	0.8	315, 358, 432 (sh), 613, [316]	320 (7000), 380 (5000), 630 (185), [293 (7100), 330 (5200)]
2.	[Cu(H_2L^2)(H_2O)] (2) green	240	60 ± 30(591.54	10.35 (10.74)	36.18 (36.51)	2.67 (2.70)	9.89 (9.47)	0.5	417, 625, [401]	306 (15,000), 325 (13,000), 394 (12,000), 660 (150), [292 (8500), 340 (6600), 352 (5600)]
3.	[Cu(H_2L^3)(H_2O)] (3) brown	230	510 ± 20(461.54)	13.38 (13.77)	52.27 (51.99)	4.75 (4.77)	12.41 (12.13)	0.3	380, 620, [326,344]	303 (35,000), 315 (32,000), 382 (26,000), 660 (168), [323 (4600)]
4.	[Cu(H_2L^4)(H_2O)] (4) light green	234	580 ± 25(533.54)	11.56 (11.95)	58.82 (58.48)	4.10 (4.12)	10.32 (10.50)	0.7	382, 436, 468 (sh), 640, [329]	328 (25,000), 382 (18,000), 425 (2000), 640 (160), [312 (5400), 327 (6200), 365 (5800), 382 (5400)]

[a] Absorption bands in the square bracket correspond to the uncoordinated ligand.

ligands exist in anti-cis configuration in DMSO-d_6 solution as deduced from ^{1}H NMR spectroscopy. Because of the anti-cis configuration, the axial carbon atoms appear downfield while the equatorial carbon atoms appear upfield. This gives rise to the same number of signals in the ^{13}C NMR spectra of the ligands as the number of carbon atoms.

3.2. Characterization of complexes

The complexes have been synthesized by template method by treating succinoyldihydrazine, $Cu(OAc)_2 \bullet H_2O$ and substituted o-hydroxyl aromatic aldehydes and ketones in 1:1:3 molar ratio in methanol.

The complexes isolated in the present study along with colour, melting point, analytical data and molar conductance have been set out in Table 1. The complexes are light green, green and brown coloured and air stable. They melt with decomposition in the temperature range 200–240 °C. All of the complexes melt with decomposition at temperatures slightly below the melting point of the corresponding ligand. This suggests that the metal–ligand bond has considerable covalent character. The complexes show no weight loss at 110 °C ruling out the possibility of presence of water molecules in their lattice. However, all of the complexes show weight loss corresponding to one water at 180 °C suggesting their presence in the first coordination sphere around the metal centre (Nikolaev et al., 1969). All of the complexes are insoluble in water and common organic solvents such as methanol, ethanol, chloroform, carbon tetrachloride, ether and benzene. They are soluble in highly coordinating solvents such as DMF and DMSO.

An effort was taken up to crystallize the complexes in various solvent systems under different experimental conditions. Unfortunately, in all our efforts, only amorphous compounds precipitated which prevented us from the analysis of the complexes by X-ray crystallization. However, the investigation of the complexes by means of electron microscopy was possible and was used to determine the morphology of the complexes (1)–(4).

The nature of the ligand seems to bear key structural factors for the morphology of the agglomerates. (Supplementary data, Figs. S1–S4) shows the agglomerate particles of the complexes. For the complexes (1) and (2), the agglomerates appear to be rod shaped which stack upon one another to give bigger agglomerates of irregular shape. The average length of the bigger agglomerates varied in the range 3375–4960 nm while the width ranged from 500 to 1200 nm. The length and width of the smaller agglomerates varied from 500 to 1375 nm and 70–375 nm, respectively. In complexes (3) and (4) also, majority of the agglomerates are of rod shaped while some appear in the form of tiny branches of the thorn. In the complex (3) some agglomerates have hexagonal shape while others have tiny spherical shape. The length and breadth of the hexagonal agglomerates are approximately 570 and 998 nm while the dimensions of the tiny spherical agglomerates are about 830 nm. The breadth and length of the rod shaped particles in complex (4) varied in the range 220–1320 nm, respectively (Afanasiev et al., 2008; Yamauchi et al., 2011). In some cases the rod shaped particles are stacked upon one another to give some particles with more irregular shape.

The size and shape of the particles have also been elucidated by TEM. The high resolution transmission electron micrographs of the complexes (1)–(4) have been shown in (Supplementary data Figs. S5–S8). The particles differ in shape and size. Majority of the particles in the complexes (1), (2) and (4) have rod shape while some of the particles appear in the form of lump consisting of spherical particles. While the bigger rods have their length in the range 1199–4025 nm and width in the range 85–400 nm, the smaller rods have length and width in the range 588–857 nm and 85–114 nm, respectively. On the other hand, the particles in the complex (3) are of spherical, hexagonal and trigonal prismatic structure. The spherical particles have dimensions in the range 4–12 nm while trigonal prismatic particles have isosceles triangular prismatic shape with dimension in the range 200 nm. The hexagonal particles are of irregular sides having length in the range 110–200 nm, respectively (Afanasiev et al., 2008; Yamauchi et al., 2011). From the shape and size of the particles in different complexes, it is evident that the methyl group present on the aldimine carbon atom has pronounced effect on the formation of the nanoparticles (Yamauchi et al., 2011) most probably, steric crowding provided by it around the metal centre.

3.3. Molar conductance

The molar conductance values for the complexes in DMSO solution at 10^{-3} M dilution are in the range 0.3–0.8 Ω^{-1} cm^2 mol^{-1}. These values are consistent with non-electrolyte nature of the complexes in this solvent (Geary, 1971).

3.4. Molecular weight

The molecular weight for the complexes was determined in DMSO solution. The experimental values of the molecular

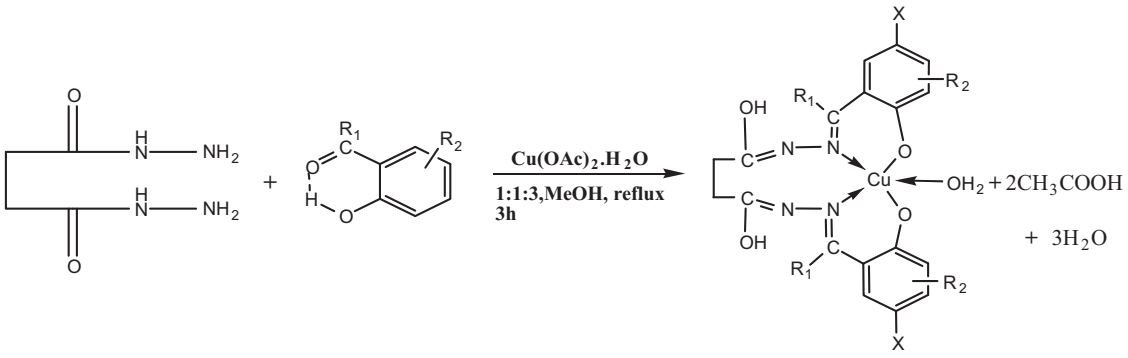

Scheme 1 Synthetic scheme for monometallic Cu(II) complexes.

weights for the complexes (1) to (4) are (480 ± 15), (660 ± 30), (510 ± 20) and (580 ± 25), respectively. These are slightly higher than the theoretical values of 433.54, 591.54, 461.54 and 533.54 for the corresponding complexes. However, these values are much less than molecular weights of the complexes corresponding to dimmer formulation and very close to the values for monomer formulation. This suggests that all of the complexes are monomer in character. Slightly higher experimental value of the molecular weights than those calculated on the basis of the monomeric formulation suggests

Table 2 Peak assignments of mass in APCI mode of some mononuclear copper complexes from succinoyldihydrazones.

Serial No	Complexes	*m/z* found	Fragment	Theoretical mass
1.	$[Cu(H_2L^1)(H_2O)](1)$	475.6	$[Cu(H_6L^1)(H_2O)_3]^+$	473.54
		491.5	$[Cu(HL^1)\bullet DMSO]^+$	492.54
2.	$[Cu(H_2L^2)(H_2O)](2)$	642	$[Cu(H_6L^2–CH_2)\ DMSO]^+$	641.54
		702	$[Cu(H_3L^2–2CH_2)\bullet 2DMSO]^+$	702.54
3.	$[Cu(H_2L^3)(H_2O)](3)$	601	$[Cu(H_4L^3)\bullet 2DMSO]^+$	601.54
4.	$[Cu(H_2L^4)(H_2O)](4)$	516	$[Cu(H_3L^4)]^+$	516.54
		594	$[Cu(H_3L^4)\bullet DMSO]^+$	594.54

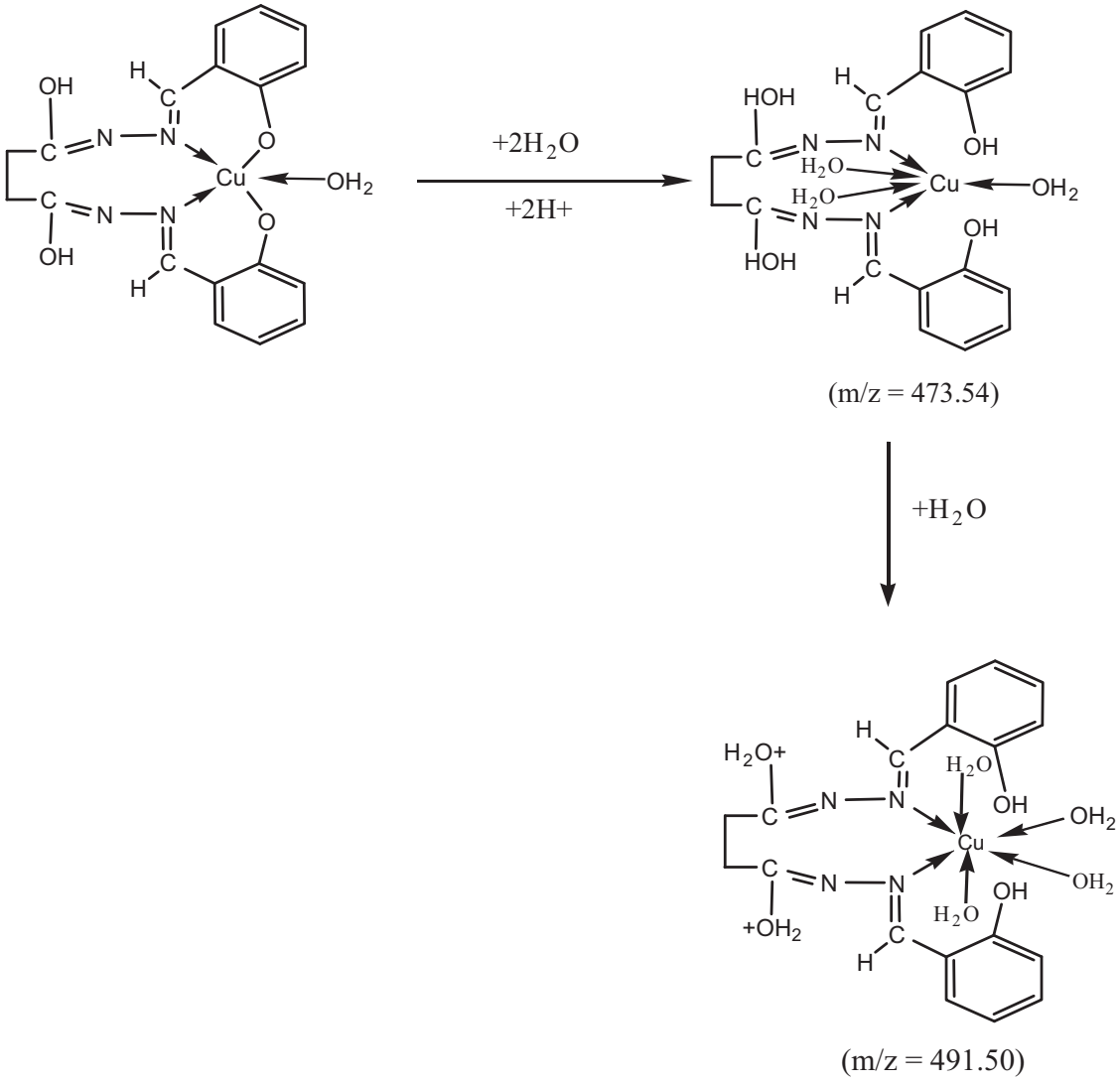

Scheme 2 Fragmentation pattern of mass spectrum of complex $[Cu(H_2L^1)(H_2O)]$(**1**).

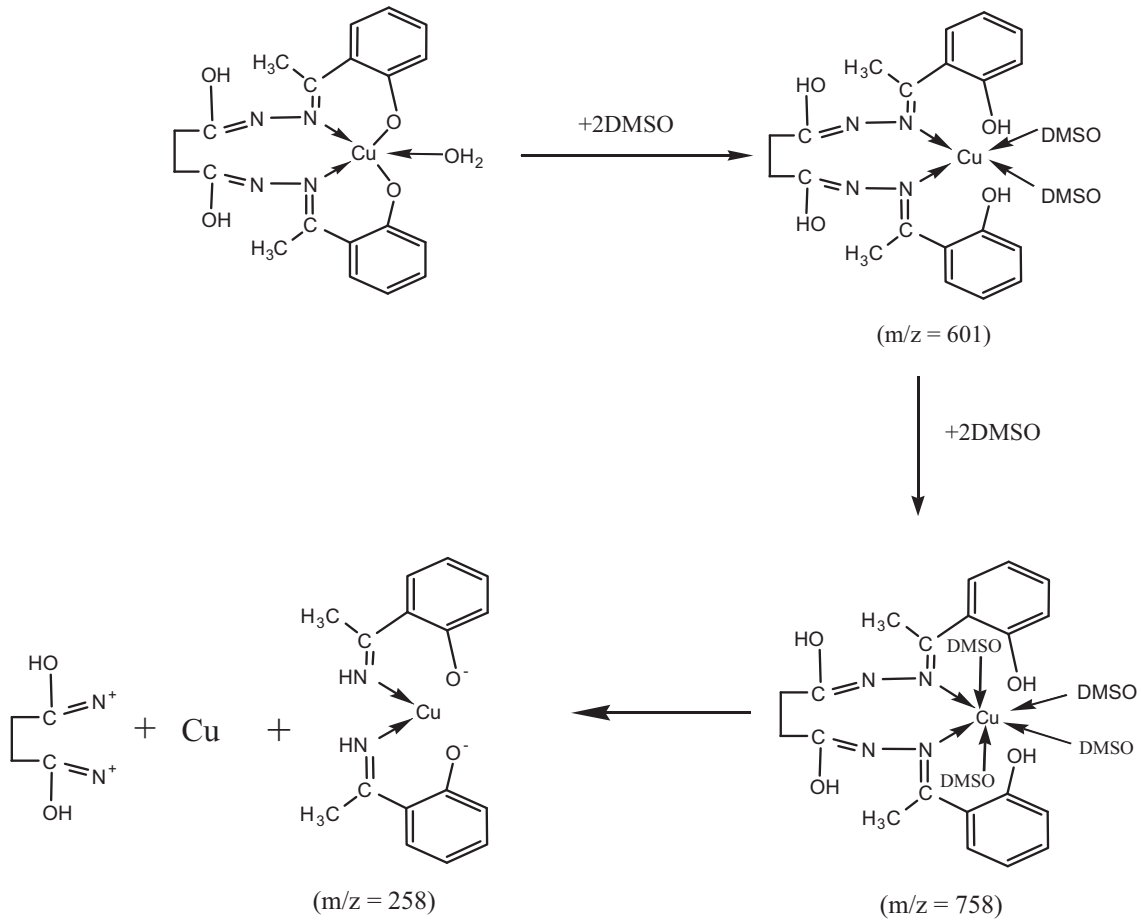

Scheme 3 Fragmentation pattern of mass spectrum of complex $[Cu(H_2L^3)(H_2O)]$(**3**).

the structure of the complexes is altered in the strongly coordinating solvents as compared to that in the solid state. Most likely, the coordinated water molecules are substituted by DMSO molecules, which accounts for higher molecular weights of the complexes (see Scheme 1).

3.5. Mass spectra

All of the complexes have been characterized by mass spectroscopy. Some prominent molecular ions along with their experimental and theoretical masses for all of the complexes have been given in Table 2. The mass spectrum of the complexes (1) and (3) is shown (Supplementary data, Figs. S9 and S10). The complexes (1) and (2) show peaks at m/z value of 491.5 and 642 respectively. These values correspond to the mass of the molecular ionic species $[Cu(HL^1)\bullet DMSO]^+$ (492.54) and $[Cu(H_6L^2–CH_2)\bullet DMSO]^+$ (641.54) which suggests that they exist in the solution under mass spectrometric conditions. The molecular ionic species $[Cu(HL^1)\bullet DMSO]^+$ in complex (1) might result from replacement of H_2O molecule by DMSO molecule while the molecular ionic species $[CuH_6L^2{-}CH_2)\bullet DMSO]^+$ in complex (2) might result from replacement of coordinated water molecule by DMSO molecule followed by loss of one methylene group from coordinated ligand. The complex (1) shows a strong peak at m/z value of 475.6. This peak originates from the molecular ion $[Cu(H_6L^1)\ (H_2O)_3]^+$ (473.54) resulting from coordination of two water molecule in solution. Further, complex (2) shows peak at m/z value of 702 corresponding to the mass of the molecular ion $[Cu(H_3L^2{-}2CH_2)\bullet 2DMSO]^+$ (702.54), respectively. The molecular ion $[Cu(H_3L^2{-}2CH_2).\ 2DMSO]^+$ originates from coordination of two DMSO molecules to the metal centre followed by loss of two $-CH_2$ groups from coordinated dihydrazone ligand. On the other hand, the complexes (3) and (4) show molecular ions at m/z values of 601 and 594, respectively. The existence of these peaks in the mass spectra of the complexes suggests the origin of the molecular ions $[Cu(H_4L^3)\bullet 2DMSO]^+$ (601.54) and $[Cu(H_3L^4)\bullet DMSO]^+$ (594.54) at m/z value of 601 and 594, respectively. These molecular ions arise from loss of coordinated water molecule followed by coordination of either one or two DMSO molecules to the metal centre (Adams et al., 1990). The complex (4) shows a peak at m/z value of 516 which may be attributed to the molecular ion $[Cu(H_3L^4)]^+$ resulted from loss of coordinated water molecule. The existence of these molecular ions in the mass spectra suggests that all of the complexes are monomer in character. It is to be noted that DMSO molecules become bonded to metal centre during recording mass spectra in DMSO solution. The fragmentation patterns of the mass spectra of the complexes are shown in Schemes 2 and 3.

Please cite this article in press as: Borthakur, R. et al., Synthesis, characterization and electrochemical properties of copper(II) complexes derived from succinoyldihydrazine Schiff base ligands. Arabian Journal of Chemistry (2015), http://dx.doi.org/10.1016/j.arabjc.2014.12.040

Table 3 Magnetic parameters for mononuclear copper complexes from succinoyldihydrazones.

Sl. No	Complex	Magnetic moment μ_{eff} (BM)	Temp	Solid /solution	$g_{\|}$ (g_3)	g_2	$g_\perp$ (g_1)	g_{av}	$A_{\|}$ (A_3)	A_2	$A_\perp$ (A_1)	A_{av}	α^2_{Cu}	R	$g_{\|}/A_{\|}$	G
1	$[Cu(H_2L^1)(H_2O)](1)$	1.83	RT	Powder	2.356	2.125	2.077	2.186	115	–	–	–	–	0.208	219.74	3.54
			LNT	Powder	2.258	2.118	2.077	2.167	–	–	–	–	–	0.239	–	
			LNT	Solution	2.298	–	2.084	2.155	170		58	95.3	0.81	–	145.0	
2	$[Cu(H_2L^2)(H_2O)](2)$	1.76	RT	Powder	2.246	–	2.104	2.151	130	–	–	–	–	–	185.6	3.13
			LNT	Powder	2.226	–	2.097	2.14	125		–	–	–	–	191.0	
			LNT	Solution	2.294	–	2.094	2.161	180	–	20	73.3	0.84	–	136.7	
3	$[Cu(H_2L^3)(H_2O)](3)$	1.85	RT	Powder	2.230	–	2.107	–	110	–	–	–	–	–	217.45	3.19
			LNT	Powder	2.322	2.111	1.988	2.140	–		80	71.7	–	–	–	
			LNT	Solution	2.204	–	2.064	2.131	168	25	60	95.8	0.75	–	143.7	
4	$[Cu(H_2L^4)(H_2O)](4)$	1.8	RT	Powder	2.204	2.064	2.054	2.107	–	–	–	–	–	0.057	–	3.42
			LNT	Powder	2.182	2.067	2.054	2.101	–	–	–	–	–	0.113	–	
			LNT	Solution	2.263	–	2.077	2.139	170		55	93.3	0.77	–	142.8	

3.6. Magnetic moment

The magnetic moment value for the complexes lies in the region 1.76–1.85 BM. This value is close to the spin only value of 1.73 BM indicating that there is no appreciable spin–spin interaction between metal atoms in the structural unit of the complexes.

3.7. Electronic spectroscopy

The electronic spectra of the complexes have been qualitatively studied in the solid state and quantitatively in DMSO solution because of the solubility reason. The positions of all the characteristic electronic absorption bands along with their molar extinction coefficient (in DMSO solution) for the complexes are given in Table 1. The solid state spectra of the complexes display an asymmetric band in the region 613–640 nm. This band is assigned to the $^2E_g \rightarrow {}^2T_{2g}$ transition. The d–d transition occurs at 800 nm in the octahedral complexes (Figgis, 1966). This band is considerably blueshifted due to Jahn–Teller distortion and in extreme case, it falls in the region 600–700 nm in square planar complexes while in the region 550–660 nm in square pyramidal complexes. The ligand field band in the region 613–640 nm having asymmetrical shape in the complexes suggests that copper centre has distorted square pyramidal stereochemistry in solid state in the complexes.

In DMSO solution, the complexes (1)–(4) have absorbance maxima in the 630–660 nm range with molar extinction coefficient in the region 150–185 $dm^3\,cm^{-1}\,mol^{-1}$. The high molar extinction coefficient in combination with asymmetrical feature of the band in the region 630–660 nm is typical of Cu(II) complexes with square pyramidal or distorted square pyramidal (McLachlan et al., 1995) geometries (d_{xz}, $d_{yz} \rightarrow d_{x^2-y^2}$). The d–d bands in DMSO solution has shifted to longer wavelength as compared to that in solid state (Karlin et al., 1982; Addison et al., 1981; Hathaway and Billing, 1970). This indicates interaction of DMSO molecule with metal centre in DMSO solution i.e. replacement of water molecule by DMSO molecules. However, the essential feature of the band in DMSO solution remains almost same as that in the solid state. This suggests that the stereochemistry of the complexes in solution as well as in the solid state remains same. The ligands show one or two very strong bands in the region 316–401 nm in the solid state which may be attributed to have combined contribution from $\pi \rightarrow \pi^*$ and $n \rightarrow \pi^*$ transition. It appears that in the solid state, the absorption bands from $\pi \rightarrow \pi^*$ and $n \rightarrow \pi^*$ transition are merged into one another giving unresolved very broad bands. However, in the solution state, the ligand bands are better resolved. The band in the region 292–312 nm may be assigned to $\pi \rightarrow \pi^*$ transition while those in the region 323–385 nm to the $n \rightarrow \pi^*$ transition. The absorption in the 303–328 nm range in all of the complexes is probably due to the intraligand $\pi \rightarrow \pi^*$ transition. Another band observed in the region 380–425 nm may be attributed to arise due to $n \rightarrow \pi^*$ transition. All the bands in the region 303–328 nm and 380–425 nm region correspond to ligand bands in the region 292–312 and 323–385 nm, respectively in the uncoordinated dihydrazone. The ligand bands are shifted to longer wavelength in the metal complexes as compared to their position in the free ligand indicating bonding between dihydrazone and metal centre. The solid state spectra of the complexes (1)

and (4) show a new band at 432 and 468 nm which may be attributed to LMCT charge transfer transition most probably, from phenolate/naphtholate oxygen atoms to the metal centre (McCollum et al., 1994) but no such bands are observable in DMSO solution.

3.8. Electron paramagnetic resonance

All of the complexes have been characterized by EPR spectroscopy at RT and LNT in powder form as well as DMSO glass at LNT. The various EPR parameters for the complexes have been set out in Table 3. The EPR spectra for the complexes (3) and (4) at LNT in solid state and in DMSO glass have been shown (Supplementary data, Figs. S11–S14).

Hamiltonian parameters $g_3/g_{||}$, g_2 and $g_1/g_{\perp}$ and hyperfine coupling constants $A_3/A_{||}$, A_2 and $A_1/A_{\perp}$ for the complexes have been included in Table 3. The complexes (1) and (4) show three g-values g_1, g_2 and g_3 in the solid state at RT as well as LNT while complex (2) shows only two g-value i.e. $g_{||}$ and $g_{\perp}$ at RT and LNT and complex (3) at LNT. On the other hand, all of the complexes show only $g_{||}$ and $g_{\perp}$ value in DMSO solution.

The intensity of the signals in the solid state spectra at RT and LNT in $g_{||}$ region rules out the possibility of either square planar or distorted octahedral stereochemistry for the complexes (1) and (4) and suggests them to have a five coordinate structure. There are two basic configurations (Jaggi et al., 1995) that can be adopted by five coordinate complexes, trigonal bipyramidal (TBP) and square pyramidal (SP). In practice, there appears to be very little difference in energy (Balhausen and Jorgenson, 1955) between the two configurations which are characterized by the ground state $d_{x^2-y^2}$ and d_z^2, respectively (Barbucci et al., 1997; Bencini and Gatteschi, 1977). The EPR spectra of Cu(II) complexes provide a very good basis for distinguishing between these ground states. Analysis of the anisotropic spectra according to Kneubuhl's method gave (Kneubuhl, 1960; Bhoon, 1983; El-Dissouky, 1983) three g-value as given in Table 3. For systems with $g_3 > g_2 > g_1$, the ratio of $(g_2 - g_1/g_3 - g_2)$ (called R parameter) is a very useful parameter for this purpose. If the ground state is predominantly d_z^2, the value of R is greater than one. On the other hand, for the ground state predominantly $d_{x^2-y^2}$, the value of R is less than one. The complexes under study have R value equal to 0.183 for (complex (1)) and 0.092 (for complex (4)). These values are less than one indicating $d_{x^2-y^2}$ as the ground state. Hence, these complexes may be suggested to have five-coordinate square-pyramidal stereochemistry (Fig. 2).

The $g_{||}$ and $g_{\perp}$ values for the copper(II) complexes (2) are 2.246 and 2.104 at RT while 2.226 and 2.097 at LNT. The complex shows copper hyperfine splitting in $g_{||}$ region both at RT and LNT with $A_{||}$ values equal to 130 and 125 G respectively. The data for both g and A are indicative of a predominantly $d_{x^2-y^2}$ ground state. The order $g_{||} > g_{\perp}$ is found for the complex both at RT and LNT. The hyperfine coupling $A_{||}$ shows weak metal–metal interaction between the metal centres.

The complex (3) shows an isotropic spectrum at RT which appears to arise due to weak intermolecular antiferromagnetic interaction between copper centres in the structural unit of the complex. However, when the temperature is lowered to LNT, the intermolecular interaction is diminished considerably

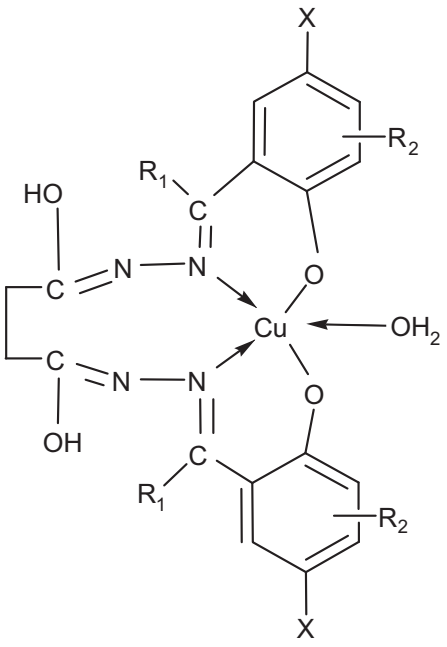

Figure 2 Suggested structure for the copper(II) complexes $[CU(H_2L^n)(H_2O)(H_4L^2 = H_4L^1, H_4L^2, H_4L^3, H_4L^4)$.

which results in the appearance of a highly anisotropic spectrum. The EPR spectrum of the complex is rhombically distorted. The highest symmetry appropriate for the CuN_2O_2 chromophore that should show rhombic splitting is C_{2v}. In this point group, both $d_{x^2-y^2}$ and d_z^2 orbitals transform to the A_1 representation (Deeth et al., 1984). Therefore, the metal part of the ground state wave function should be mixture of both these orbitals.

Three possible mechanisms have been suggested (McGarvey, 1966), which can split g_x and g_y. These are (1) difference in the E_{xy} and E_{yz} values where E_{xy} is the energy difference between the ground state and d_{xy} and so on, (2) difference in the reduction factors (excited state delocalization) and (3) magnitude of coefficients of $d_{x^2-y^2}$ and d_z^2 in the ground state function, respectively.

Detailed calculation on Cu(II)-doped Zn(1,2-dimethylimidazole)$_2$Cl$_2$ host lattice having a pseudo-tetrahedral structure (Gewith et al., 1987) suggest that for a difference of ca. 125 nm between E_{xy} and E_{yz} values, the difference $(g_x - g_y)$ can be as much as 0.04. In the absence of polarized electronic spectral data, it is not possible to designate the ligand field transitions observed. Hence, point (1) above cannot account for such large splitting in the g-value ($g_x = 1.988$, $g_y = 2.111$, $g_z = 2.322$). The major contributing factors towards the rhombic splitting for complex (3) should be either due to d_z^2 mixing into the ground state wave functions or extensive excited state delocalization or both.

Belford et al. (Hitchmaun et al., 1969), defined a parameter Rg to evaluate the extent of d_z^2-mixing into the ground state, neglecting the orbital reduction factor. The factor Rg is measure of the degree of rhombic splitting in the g-value. The Rg factor calculated for the complex (3) in the present study is 2.61. Rg is 0.9 for stellocyamin while for Cu(II)-doped Zn(1,2-dimethylimidazole)Cl_2, this value is 1.1. The Rg

parameter is a steep function of the extent of d_z^2 mixing in the ground state which implies that rhombic splitting should be sensitive to the amount of d_z^2 mixed into the ground state. The value of 2.61 for *Rg* suggests a mixing of d_z^2 into the ground state to the extent of about 7.1%. However, for the copper(II) doped zinc complex above ca. 3% mixing is suggested for the observed *g* split (0.102). The split observed between g_x and g_y in the present case is 0.123. On this basis, the mixing of d_z^2 into the ground state is suggested to be 3.63% which is almost half that suggested on the basis of *Rg* parameter. Further, for a 4–5% mixing, the difference between A_x and A_y should be $60 \times 10^{-4}\,cm^{-1}$. The spectrum of the complex (3) showed metal-hyperfine splitting in the g_x and g_y region which comes out to be 25 and 85 G, respectively. Hence, the difference between A_x and A_y comes out to be $51.28 \times 10^{-4}\,cm^{-1}$. This difference suggests mixing of d_z^2 orbital into the ground state to the extent of 3.4–4.3%. Considering both these factors together, it appears pertinent to suggest that the mixing to the extent of 3.8–4.0% of d_z^2 occurs into the ground state. It is quite reasonable to assume that the *Rg* parameter defined by Belford et al. (Hitchmaun et al., 1969) overestimate the mixing of d_z^2 orbital into the ground state and hence it is not true parameter in the present case. Consequently, the possibility of mixing of d_z^2 orbital into ground state to the extent of about 7% suggested by *Rg* parameter is discarded. The superhyperfine structure in the g_z region is observed on the highest field signal in the complex. Clearly five superhyperfine lines are observed for the complex suggesting two nitrogen atoms in the coordination sphere. The superhyperfine coupling constant is $A_{||N} = 19$ G. This corresponds to coupling of electron spin with the nuclear spin of two nitrogens (Vogel, 1978). This indicates coordination of two nitrogen atoms of dihydrazone ligand to the metal centre. In frozen DMSO solution, all of the copper(II) complexes show axial spectra, the g factors and A constants are summarized in Table 3. The data for both *g* and *A* are indicative of a predominantly $d_{x^2-y^2}$ ground state. The order $g_{||} > g_\perp$ and $A_{||} > A_\perp$ is found for all complexes studied.

It is well known that a pseudo-tetrahedral distortion leads to a greatly reduced value of $A_{||}$ and an increased value of $g_{||}$. Often the ratio $g_{||}/A_{||}$ has been empirically treated as an index of tetrahedral distortion in square planar complexes. However, in case of octahedral or square-pyramidal complexes, this has been related to the increased distortion in the equatorial plane. For square-planar structures the usual range is 105–135 and for tetrahedral distorted complexes, it is 150–250 (Sakaguchi and Addison, 1979). $g_{||}/A_{||}$ quotients for the complexes (2) and (3) fall in the region 185–215 in the solid state. Such a large value for $g_{||}/A_{||}$ quotients for the complexes is suggested to reflect the increased distortion in the equatorial plane (Kivelson and Neiman, 1961). This clearly reflects a lower symmetry for the complexes (Syamal et al., 1979) in solid state. In the complexes the $g_{||}/A_{||}$ in DMSO glass falls in the region 136.7–145.0. This value suggests that there is either no distortion or negligible distortion in the equatorial plane of the complexes in the DMSO solution.

The in-plane covalency parameter α^2_{Cu} was calculated for the copper (II) complexes using the equation given by Kivelson and Neiman (Ahmed et al., 1966; Ahmed and Chaudhuri, 1969). Values obtained are listed in Table 3. The α^2_{Cu} values for the complexes are 0.75–0.92 < 1, indicating that the complexes have some covalent character. The nature of the ligand forming the complex is evaluated from *G*-value obtained using the following equation

$$G = g\| - 2/g\perp - 2$$

.

When $G < 4.0$, the ligand forming complex is regarded as strong field. For square planar complexes, *G* is usually in the region 2.03–2.45 (Kumar et al., 2011). *G*-values for the present complexes are 3.13–3.54, suggesting that the dihydrazones have moderately strong ligand field strength in the complexes. On the basis of the magnitude of *G*-parameter, it may be suggested that the ligand field strength for the dihydrazone increases in the order $H_4L^1 < H_4L^4 < H_4L^3 < H_4L^2$. Further, if $G > 4.0$, the local tetragonal axes are aligned parallel or only slightly misaligned. If $G < 4.0$, significant exchange coupling is present and the misalignment is appreciable. The observed *G*-values for the exchange interaction parameter for the complexes ($G = 3.13$–3.54) suggest that the local tetragonal axes are misaligned and the unpaired electron is in the $d_{x^2-y^2}$ orbital.

3.9. Infrared spectra

Some structurally significant IR bands for uncoordinated dihydrazone and complexes have been set out in Table 4. The free succinoyldihydrazine shows relatively strong bands at 3300, 3200 and 1652 cm^{-1}. The bands at 3300 and 3200 are assigned to arise due to νNH vibrations of secondary —NH and primary —NH_2 groups respectively. The band at 1652 cm^{-1} originates from joint contribution of stretching vibrations of >C═O groups and bending vibrations of NH_2 groups, respectively (Dyer, 1989). The essential features of these bands suggest that >C═O and —NH_2 groups of dihydrazine are involved in strong intramolecular H-bonding. The reaction of $Cu(OAc)_2 \bullet H_2O$ with succinoyldihydrazide in 1:1 molar ratio in methanol followed by reaction with o-hydroxy aromatic aldehydes and ketones keeping $Cu(OAc)_2 \bullet H_2$ O:SDH: o-hydroxy aromatic aldehydes and ketones molar ratio at 1:1:3 yields the complexes (1)–(4). The complexes show IR spectral features entirely different from that of succinoyldihydrazine yet some similarity with that of uncoordinated dihydrazone. The complexes show a medium to strong broad band in the region 3100–3500 cm^{-1} with their centres in the range 3424–3446 cm^{-1} bears similarity with the band in the region 3428–3434 cm^{-1} in preformed dihydrazone. The band in the region 3428–3434 cm^{-1} is similar in its essential feature to the bands observed in organic alcohols (Nakamoto, 1986; Nakagawa and Shimanouchi, 1964) in the same region. Hence, the bands in the region 3100–3500 cm^{-1} in uncoordinated dihydrazones and metal complexes are attributed to arise due to νOH vibration of —OH groups. This shows the presence of —OH groups in the complexes. This band may be attributed to stretching vibrations of —OH group present in coordinated ligand generated as a result of enolization and coordinated H_2O molecules. The weight loss corresponding to one water molecule at 180 °C corroborates unambiguously the fact that this water molecule is coordinated to metal centre. On the basis of theoretical calculations, it has been suggested that rocking, wagging and metal–oxygen stretching vibrations appear at 900, 768 and 673 cm^{-1}.

Please cite this article in press as: Borthakur, R. et al., Synthesis, characterization and electrochemical properties of copper(II) complexes derived from succinoyldihydrazine Schiff base ligands. Arabian Journal of Chemistry (2015), http://dx.doi.org/10.1016/j.arabjc.2014.12.040

Table 4 Structurally significant Infrared (IR) bands (in cm^{-1}) for succinoyldihydrazones and their Cu(II) complexes.

Sl. No.	Ligand/complex	ν(OH + NH)	ν(C═O)	ν(C═N)	Amide II + (C─O) (phenyl/naphthyl)	ν(NCO─)	ν(C─O)	ν(N─N)	(M─O) (phenolic)
	(H_4L^1)	3428 (s) 3203 (s)	1662 (s)	1611 (s) 1623 (s)	1566 (s)	–	1269(s)	1033(s)	–
	(H_4L^2)	3431 (m) 3192 (s)	1662 (vs)	1615 (s)	1560 (m)	–	1267(s)	1045 (wsh)	–
	(H_4L^3)	3435 (s) 3205 (s)	1685 (s)	1600 (s) 1621 (ssh)	1540 (s)	–	1300 (m)	1036 (w)	–
	(H_4L^4)	3434 (m) 3227 (s)	1670 (s) 1640 (s)	1620 (s)	1530 (s)	–	1280 (s)	1031(m)	–
1.	$[Cu(H_2L^1)(H_2O)](1)$	3433 (s)	–	1618 (s)	1533 (s)	1510 (vs)	1301 (m) 1278 (m)	1034 (w)	544 (w)
2.	$[Cu(H_2L^2)(H_2O)](2)$	3431 (s)	–	1617 (s)	1540 (m)	1511 (vs)	1302 (m) 1268 (m)	1030 (w)	548 (w)
3.	$[Cu(H_2L^3)(H_2O)](3)$	3433 (s)	–	1600 (s)	1530 (ssh)	1510 (msh)	1307 (msh) 1290 (s)	1035 (w)	570 (w)
4.	$[Cu(H_2L^4)(H_2O)](4)$	3446 (s)	–	1618 (s) 1603 (s)	1539 (s)	1520 (s)	1300 (m)	1038 (w)	575 (w)

However, these frequencies are sensitive to the strength of coordinate bond as well as hydrogen-bonding in crystals. On comparing the IR spectra of complexes with those of the uncoordinated ligands in the region below 1000 cm^{-1}, new weak bands have been observed in the 844–870 and 670–690 cm^{-1} regions, respectively. As these bands are not observed in the IR spectra of the ligands, hence they are attributed to rocking and wagging vibrations of water molecules bonded to the metal centre (Young et al., 1996) respectively. Another important and most characteristic feature of the IR spectrum of the complexes is the absence of the band in the region 1630–1700 cm^{-1} due to >C═O groups and bending vibration of NH_2 groups. The complexes show a new band in the region 1618 cm^{-1} which is similar in nature to the band in the region 1600–1625 cm^{-1} in the free ligands and falls in the region in which coordinated >C═N group in hydrazone metal complexes have been reported to absorb. Hence, this band is assigned to ν(C═N) (Mashiuca, 1962). All these pieces of evidences suggest that NH_2 group of dihydrazine and >C═O group of o-hydroxy aromatic aldehydes and ketones condense generating the dihydrazone in metal complexes (Vogel, 1978). Further, the intensity of the ν(C═N) band is increased as compared to the corresponding band in the free dihydrazone. This is due to the reinforcement of the intensity of the ν(C═N) band due to newly created >C═N─N═C< group. Another important feature of the IR spectra of the complexes is that they show a new weak to strong band in the region 1510–1520 cm^{-1}. This band is characteristic of the presence of NCO^- group (Syamal and Kale, 1979). The essential feature associated with this band in the IR spectrum of the complexes suggests that the dihydrazones undergo enolization.

The complexes show a band in the region 1268–1307 cm^{-1} which corresponds to the strong band in the region 1269–1280 cm^{-1} in the free ligand dihydrazone due to ν(C─O) (phenolic/naphtholic). The shift of this band to higher frequency by 3–29 cm^{-1} indicates bonding of phenolic/naphtholic oxygen atom to the metal centre via deprotonation (Percy and Thornton, 1972). The complexes show new bands in the region 544–575 cm^{-1} which are assigned to ν(M─O)(phenolate/naphtholate) (Nakamoto et al., 1970). Further, the absence of any band in the region 445–480 cm^{-1} rules out the absence of bond formation between enolate oxygen atoms and metal centre (Cameron and Brooker, 2011).

3.10. Cyclic voltammetry

Cyclic voltammetric studies of the complexes and ligand are performed in DMSO solution containing TBAP as supporting electrolyte. The three electrode cell is equipped with a glassy carbon working electrode, a platinum wire auxiliary electrode and a Ag/AgCl reference electrode. The cyclic voltammetric data have been given in Table 5. The cyclic voltammogram for the complexes (1)–(4) has been shown in (Supplementary data, Figs. S15–S18).

On comparing the CV of the complexes with the corresponding dihydrazone ligand, it is concluded that all of the complexes show two metal centred electron transfer reactions. With the highly negative charged dihydrazone ligand bonded to the metal centre, it is expected to help make the reduction of these metal centres unfavourable, leading to quite negative E_{pc} values (Okawa et al., 1988).

Please cite this article in press as: Borthakur, R. et al., Synthesis, characterization and electrochemical properties of copper(II) complexes derived from succinoyldihydrazine Schiff base ligands. Arabian Journal of Chemistry (2015), http://dx.doi.org/10.1016/j.arabjc.2014.12.040

Table 5 Electrochemical data of mononuclear copper complexes from succinoyldihydrazones at a scan rate of 100 mV/s.

Sl. No.	Complex	E_{pc} (V)	E_{pa} (V)	Redox couple	ΔE (mV)
1	$[Cu(H_2L^1)(H_2O)]$	–	+0.53	Second >C═N group	70
		–	+0.18	Cu^{III}/Cu^{II}	
		−0.29	−0.22	Cu^{II}/Cu^{I}	
		−0.94	–	Dihydrazone centred	
		−1.45	–	Dihydrazone centred	
2	$[Cu(H_2L^2)(H_2O)]$	–	+0.65	Second >C═N group	270
		−0.32	−0.05	Cu^{II}/Cu^{I}	
		−0.77	–	Dihydrazone centred	
		−1.41	–	Dihydrazone centred	
3	$[Cu(H_2L^3)(H_2O)]$	–	+1.08	First >C═N group	220
		–	+0.75	Second >C═N group	
		–	+0.17	Cu^{III}/Cu^{II}	
		−0.37	−0.15	Cu^{II}/Cu^{I}	
		−0.82	–	Dihydrazone centred	
		−1.38		Dihydrazone centred	
4	$[Cu(H_2L^4)(H_2O)]$	–	+1.24	First >C═N group	80
		–	+0.60	Second >C═N group	
		−0.25	−0.17	Cu^{II}/Cu^{I}	
		−0.93	–	Dihydrazone centred	
		−1.37	–	Dihydrazone centred	

In the reductive scan all the complexes show three well defined reductive waves at a scan rate of 100 mV/s. On the reverse sweep, the complexes (1) and (4) show three oxidative waves each while the complexes (2) and (3) show two and four oxidative waves each, respectively. Complexes show either one or two reductive waves in the region (−0.94) to (−0.77 V) and (−1.45) to (−1.37 V), respectively. These reductive waves do not have their counterparts in the return scan. This suggests that the species produced corresponding to these reductive waves are unstable in DMSO solution and revert back to the original species. These waves may be attributed to ligand centred electron transfer reductive reactions. Further, the oxidative wave is observed in the region +1.08 to +1.24 V which is attributed to oxidation of first >C═N group, that in the region +0.53 to +0.75 V is attributed to oxidation of second >C═N group, respectively. The remaining reductive and oxidative waves may be attributed to metal centred electron transfer reactions. The first redox couple ($E_{1/2}$ = −0.26 V, E_{pa} = −0.22 V and E_{pc} = −0.29 V in complex (1) ($E_{1/2}$ = −0.21 V, E_{pa} = −0.17 V and Ep_c = −0.25 V in complex (4))) is reversible. The peak potential separation is ΔEp = 70 mV and 80 mV, respectively, and the ratio of cathodic to anodic peak currents is close to unity. This wave may be assigned to Cu^{II}/Cu^{I} redox couple. The complex (1) shows another oxidative wave at +0.18 V as well. This wave does not have its counterpart in the reductive wave. This suggests that the metal centred species corresponding to this wave is again unstable in solution and reverts back to the original species. Hence, this irreversible oxidation wave may be assigned to the oxidative couple Cu^{III}/Cu^{II}.

Apart from the reductive waves in the regions (−0.77) to (−0.82 V) and (−1.38) to (−1.41 V) due to ligand centred electron transfer reactions, the complexes (2) and (3) in the forward scan show a reductive wave at −0.32 and −0.37 V, respectively. This reductive wave may be assigned to electron transfer reaction centred on the metal. The corresponding oxidative waves appear at −0.05 and −0.15 V, respectively, in return scan. The reductive and oxidative waves are separated from one another by 270 and 220 mV, respectively, suggesting that the redox processes are either irreversible or quasi-reversible in nature. The high peak separation, most probably, originated from a slow heterogeneous electron exchange rate rather than from interfering homogeneous reaction (Percy and Thornton, 1972). The complex (3) shows another irreversible oxidative wave at +0.17 V similar to that in the complex (1). Hence, this oxidative wave may be attributed to oxidative couple corresponding to oxidation of Cu^{II} to Cu^{III}. In view of this, the first redox couple (E_{pc} = −0.37, Ep = −0.15 V) in complex (3) may be attributed to the reduction of Cu^{II} to Cu^{I}. As the separation between cathodic and anodic waves for the first redox couple is large and the complex (3) shows two metal centred electron transfer reactions, it is imperative to assume that the single redox couple in complex (2) arises from Cu^{II}/Cu^{I} redox couple. In order to confirm that the electron transfer reaction in the complexes (2) and (3) is a quasi-reversible metal centred electron transfer reaction and the large separation between reductive and oxidative waves is due to slow heterogeneous electron exchange only, the cyclic voltammogram of the complexes was recorded at scan rates of 150 mV/s and 50 mV/s also. The cyclic voltammogram of the complexes (2) and (3) at scan rate of 150 mV/s has essentially the similar feature as that at 100 mV/s. As above, the complexes (2) and (3) show reductive wave at −0.30 and −0.32 V while the oxidative wave at 0.00 and −0.08 V, respectively. The difference between the redox couples is 300 and 240 mV, respectively. However, both the complexes gave better resolved cyclic voltammograms at 50 mV/s than that obtained at 100 mV/s. In both the complexes (2) and (3), the cyclic voltammograms show almost similar essential features. Apart from the reductive waves at −0.69, −1.26

Please cite this article in press as: Borthakur, R. et al., Synthesis, characterization and electrochemical properties of copper(II) complexes derived from succinoyldihydrazine Schiff base ligands. Arabian Journal of Chemistry (2015), http://dx.doi.org/10.1016/j.arabjc.2014.12.040

and −0.73 due to ligand centred electron transfer reactions, complexes (2) and (3) show reductive waves at −0.31 and −0.21 V and oxidative waves at −0.25, +0.12 and −0.15 and +0.21 V, respectively. The reductive waves at −0.31 (complex 2) and −0.21 V (complex 3) correspond to the oxidative waves at −0.25 and −0.15 V, respectively. The ratio between the cathodic peak current and the square root of the scan rate ($I_{pc}/\nu^{1/2}$) is constant for the first redox couple. The peak potential shows a small dependence upon the scan rate. The ratio I_{pc}/I_{pa} is 0.9 which is close to unity (West et al., 1993). On comparing the earlier data with the observed data (Okawa et al., 1988) it can be deduced that this redox couple is related to either quasi-reversible or reversible one electron transfer process controlled by diffusion (Donzello et al., 2003).

For the first redox couple, the point of crucial importance is that when the scan rate is decreased from 150 mV/s to 100 mV/s to 50 mV/s, the position of the peaks changes and separation between them decreases from 300 to 270 to 60 mV for the complex (2) and from 150 to 80 to 60 for the complex (4). Such a cyclic voltammetric behaviour of the complexes shows that this is a quasi-reversible electron transfer process. However, this electron transfer becomes completely reversible at a scan rate of 50 mV/s. Further, these complexes show another oxidative wave as well at +0.12 and +0.23 V at a scan rate of 50 mV. This wave is similar to the second oxidative wave observed in the complexes (1). Hence, this may be attributed to Cu^{III}/Cu^{II} redox couple corresponding to oxidation of Cu^{II} to Cu^{III}. However, this oxidative wave does not have its counterpart in the cathodic scan. This suggests that the Cu^{III} species produced in the reaction is transient and returns back to its original species. The electrode reactions corresponding to these redox waves may be shown below

$$[Cu^{III}(H_2L)(H_2O)]^+ \underset{-e}{\overset{+e}{\rightleftharpoons}} [Cu^{II}(H_2L)(H_2O)] \underset{-e}{\overset{+e}{\rightleftharpoons}} [Cu^{I}(H_2L)(H_2O)]^-$$

4. Conclusions

In the present study, we have synthesized four mononuclear copper(II) complexes of composition $[Cu(H_2L^n)(H_2O)]$ by template method in excellent yield. All of the complexes are monomeric and non-electrolyte. The ligands are present in enol form in all of the complexes and function as dibasic tetradentate ligand coordinating to the metal centre through phenolate/naphtholate oxygen atoms and azomethine nitrogen atoms. The agglomerates in complexes (1), (2) and (4) appear to be rod shaped while in complex (3) agglomerates have hexagonal as well as spherical shape. The majority of the nanoparticles in complexes (1), (2) and (3) are rod shaped while some of the particles appear in the form of lump of spherical shape. The EPR parameters indicate that the copper centre has $d_{x^2-y^2}$ orbital as the ground state. All of the complexes showed two metal centred electron transfer reactions in the cyclic voltammetric studies. On the basis of physico-chemical and spectroscopic data the complexes are suggested to have distorted square pyramidal stereochemistry.

Acknowledgements

Authors are thankful to the HEAD, SAIF, North Eastern Hill University, Shillong-793022, Meghalaya, India for recording mass spectra, the Head, SAIF, IIT Bombay, India for recording EPR spectra. Authors express their heartfelt thanks to Prof. A.T. Khan, Department of Chemistry, IIT Guwahati, Assam, India for helping in recording the magnetic moment data.

Appendix A. Supplementary material

Supplementary data associated with this article can be found, in the online version, at http://dx.doi.org/10.1016/j.arabjc.2014.12.040.

References

Adams, H., Bailey, N.A., Crane, J.D., Feuton, D.E., Latour, J.-M., Williams, J.M., 1990. J. Chem. Soc., Dalton Trans., 1727
Addison, A.W., Hendriks, H.M.J., Reedijk, J., Thompson, L.K., 1981. Inorg. Chem. 20, 103.
Afanasiev, P., Chouzier, S., Czeri, T., Pilet, G., Pichon, C., Roy, M., Vrinat, M., 2008. Inorg. Chem. 47, 2303.
Ahmed, A.D., Chaudhuri, N.R., 1969. J. Inorg. Nucl. Chem. 31, 2545.
Ahmed, A.D., Mandal, P.K., Chaudhuri, R., 1966. J. Inorg. Nucl. Chem. 28, 2951.
Ajaikumar, S., Pandurangan, A., 2008. J. Mol. Catal. A Chem. 290, 35.
Balhausen, C.J., Jorgenson, C.J., 1955. Kgl Donske Vendenskab Selskab Met Esy Medd 29, 14.
Barbucci, R., Bencini, A., Gatteschi, D., 1997. Inorg. Chem. 16, 2117.
Bencini, B.A., Gatteschi, D., 1977. Inorg. Chem. 16, 1994.
Bhoon, Y.K., 1983. Ind. J. Chem. 22A, 430.
Cameron, S.A., Brooker, S., 2011. Inorg. Chem. 50, 3697.
Chanu, O.B., Kumar, A., Ahmed, A., Lal, R.A., 2012a. J. Mol. Struct. 1007, 257.
Chanu, O.B., Kumar, A., Lemtur, A., Lal, R.A., 2012b. Spectrochim. Acta A 96, 354.
Choudhary, V.R., Dumbre, D.K., Uphade, B.S., Narkhede, V.S., 2004. J. Mol. Catal. A Chem. 215, 129.
Deeth, R.J., Hitchman, M.A., Lehman, G., Sachs, H., 1984. Inorg. Chem. 33, 1310.
Dinda, R., Sengupta, P., Ghosh, S., Sheldrick, S., 2003. Eur. J. Inorg. Chem., 363
Donzello, M.P., Dini, D., Arcangelo, G.D., Frcolani, C., Zhan, R., Qu, Z., Stuzhin, P.A., Kadish, K.M., 2003. J. Am. Chem. Soc. 125, 14190.
Dyer, J.R., 1989. Applications of Absorption Specrtroscopy of Organic Compounds. Prentice Hall of India Pvt Ltd, New Delhi.
El-Dissouky, A., 1983. Ind. J. Chem. 22A, 427.
Figgis, B.N., 1966. Introduction to Ligand Fields. Wiley.
Geary, W.J., 1971. Coord. Chem. Rev. 7, 81.
Gewith, A.G., Cohen, S.L., Schugar, H.J., Solomon, E.I., 1987. Inorg. Chem. 36, 1133.
Gourlay, C., Nielsen, D.J., White, J.M., Knottenbelt, S.Z., Kirk, M.L., Young, C.G., 2006. J. Am. Chem. Soc. 128, 2164.
Hathaway, B.J., Billing, D.E., 1970. Coord. Chem. Rev. 5, 143.
Hitchmaun, M.A., Oilson, C.D., Betford, R.L., 1969. J. Chem. Phys. 50, 1195.
Jackman, L.M., Sternhell, S., 1978. Application of Nuclear Magnetic Resonance Spectroscopy in Organic Chemistry, Vol. 10, second ed. Pergamon Press, Amsterdam (Chapter 3).
Jaggi, A., Chandra, S., Sharma, K.K., 1995. Polyhedron 4, 163.
John, R.P., Park, M., Moon, D., Lee, K., Hong, S., Zou, Y., Lah, M.S., 2007. J. Am. Chem. Soc. 129, 14142.
Karlin, K.D., Hayes, J.C., Juen, S., Hutchinson, J.P., Zubieta, J., 1982. Inorg. Chem. 21, 4106.

Kato, C.N., Hasegawa, M., Sato, T., Yoshizawa, A., Inoue, T., Mori, W., 2005. J. Catal. 230, 226.
Kivelson, D., Neiman, R., 1961. J. Chem. Phys. 35, 149.
Kneubuhl, F.K., 1960. J. Chem. Phys. 33, 1074.
Kumar, A., Lal, R.A., Chanu, O.B., Borthakur, R., Koch, A., Lemtur, A., Adhikari, S., Choudhury, S., 2011. J. Coord. Chem. 64, 1742.
Lal, R.A., Choudhury, S., Ahmed, A., Chakraborty, M., Borthakur, R., Kumar, A., 2009. J. Coord. Chem. 62, 3864.
Lal, R.A., Choudhury, S., Ahmed, A., Borthakur, R., Asthana, M., Kumar, A., 2010a. Spectrochim. Acta A 75, 212.
Lalami, N.A., Manfred, H.H., Noli, H., Meyer, P., 2011. Trans. Met. Chem. 36, 669.
Mashiuca, M., 1962. Bull. Chem. Soc. Jpn. 35, 2020.
McCollum, D.G., Hall, L., White, C., Ostvauder, R., Rheingold, A.L., Whelan, J., Bosnich, B., 1994. Inorg. Chem. 33, 924.
McGarvey, R., 1966. Trans. Met. Chem. 3, 89.
McLachlan, G.A., Fallon, G.D., Martin, R.L., Spiccia, L., 1995. Inorg. Chem. 34, 254.
Nakagawa, I., Shimanouchi, T., 1964. Spectrochim. Acta A 20, 429.
Nakamoto, K., 1986. Infrared and Raman Spectra of Inorganic and Coordination Compounds. John Wiley & Sons, New York.
Nakamoto, K., Udovich, C., Takamoto, J., 1970. J. Am. Chem. Soc. 92, 3973.
Nikolaev, A.V., Logvienko, V.A., Myachina, L.I., 1969. Thermal Analysis. Academic Press, New York.
Okawa, H., Koikawa, M., Kida, S., 1988. J. Chem. Soc. Dalton Trans., 641
Percy, G.-C., Thornton, D.A., 1972. J. Inorg. Nucl. Chem. 34, 3369.
Perez, Y., Ballesteros, R., Fajardo, M., Sierra, I., del Hierro, I., 2012. J. Mol. Catal. A Chem. 352, 45.
Ranford, J.D., Vittal, J.J., Wang, Y.M., 1998. Inorg. Chem. 37, 1226.
Sakaguchi, V., Addison, A.W., 1979. J. Chem. Soc., Dalton Trans., 600
Siegel, A., Siegel, H., 2002. Metal Ions in Biological Systems. Marcel Dekker, New York.
Solomon, E.I., Sundaram, U.M., Machonkin, T.E., 1996. Chem. Rev. 96, 2563.
Solomon, E.I., Szilagyi, R.K., George, S.D., Basumallick, L., 2004. Chem. Rev. 104, 419.
Syamal, A., Dutta, R.L., 1993. Elements of Magnetochemistry. East-West Press Pvt Ltd, New Delhi.
Syamal, A., Kale, K.S., 1979. Inorg. Chem. 18, 992.
Valodkar, V.B., Tembe, G.L., Ravindranathan, M., Ram, R.N., Rama, H.S., 2004. J. Mol. Catal. A Chem. 208, 21.
Vogel, A.I., 1978. A Textbook of Quantitative Inorganic Analysis Including Elementary Instrumentation Analysis. ELBS and Longmans, London.
West, P.X., Liberta, E., Padhye, S.B., Chikate, R.C., Sonawave, P.B., Kumbrar, A.S., Yerravda, R.S., 1993. Coord. Chem. Rev. 123, 49, and references therein.
Xavier, K.O., Chacko, J., Yusuff, K.K.M., 2004. Appl. Catal. A Gen. 258, 251.
Yamauchi, T., Tsukahara, Y., Yamada, K., Sakata, K., Wada, Y., 2011. Chem. Mater. 23, 75.
Young, Y., Foung, R., Fu, K., 1996. Polyhedron 15, 3753.

Please cite this article in press as: Borthakur, R. et al., Synthesis, characterization and electrochemical properties of copper(II) complexes derived from succinoyldihydrazine Schiff base ligands. Arabian Journal of Chemistry (2015), http://dx.doi.org/10.1016/j.arabjc.2014.12.040